Directed evolution of sequence-regulating polyhydroxyalkanoate synthase to synthesize medium-chain-length-short-chain-length (MCL-SCL) block copolymer

Hien Thi Phan,[1] Yumi Hosoe,[1,‡] Maureen Guex,[2,‡] Masayoshi Tomoi,[3,‡†] Hiroya Tomita,[4] Manfred Zinn,[2] and Ken'ichiro Matsumoto[4,]*

[1]Graduate School of Chemical Sciences and Engineering, Hokkaido University, Sapporo, Japan, [2]Institute of Life Technologies, University of Applied Sciences and Arts Western Switzerland (HES-SO Valais-Wallis), Sion, Switzerland, [3]Course of Applied Chemistry, Department of Engineering, Hokkaido University, Sapporo, Japan, [4]Division of Applied Chemistry, Faculty of Engineering, Hokkaido University, Sapporo, Japan

KEYWORDS: PHA synthase, in vitro evolution, poly(3-hydroxybutyrate), sequence regulation, biodegradable plastic

ABSTRACT: Sequence-regulating polyhydroxyalkanoate synthase $PhaC_{AR}$ is a chimeric enzyme comprising PhaCs from *Aeromonas caviae* and *Ralstonia eutropha* (*Cupriavidus necator)*. It spontaneously synthesizes short-chain-length (SCL, ≤ C_5) block copolymer poly(2-

hydroxybutyrate)-*b*-poly(3-hydroxybutyrate) [P(2HB)-*b*-P(3HB)] from a mixture of monomer substrates. In this study, directed evolution of $PhaC_{AR}$ was performed to increase its activity toward a medium-chain-length (MCL, $C_{6–12}$) monomer, 3-hydroxyhexanoyl (3HHx)-coenzyme A (CoA). Random mutagenesis and selection based on P(3HB-*co*-3HHx) production in *Escherichia coli* found that the beneficial mutations N149D and F314L increase the 3HHx fraction. The site-directed saturation mutagenesis at the position 314, which is adjacent to the catalytic center C315, demonstrated that F314H synthesizes P(3HHx) homopolymer. The F314H mutant exhibited increased activity toward 3HHx-CoA compared with the parent enzyme, whereas the activity toward 3HB-CoA decreased. The predicted tertiary structure of $PhaC_{AR}$ by AlphaFold2 provided insight on the mechanism of the beneficial mutations. In addition, this finding enabled to synthesize a new PHA block copolymer, P(3HHx)-*b*-P(2HB). Solvent fractionation indicated the presence of a covalent linkage between the polymer segments. This novel MCL-SCL block copolymer considerably expands the range of the molecular design of PHA block copolymers.

Introduction

Polyhydroxyalkanoates (PHAs) are microbial polyesters produced as intracellular carbon and energy storage. In natural PHA producers, polymer synthesis is promoted under nitrogen and/or phosphorus limited conditions with an excess of carbon[1]. Recombinant *Escherichia coli*, however, produced PHA on nutrient-rich medium containing excess carbon sources.[2] Some PHAs possess thermoplastic properties and are useful as biobased alternatives to petroleum-derived plastics. Various applications of the material is being investigated.[3] Given the severity of oceanic plastic pollution, the superior biodegradability of PHA has attracted significant research interest.[4,5]

PHA monomeric units are categorized into short-chain-length (SCL, $\leq C_5$) and medium-chain-length (MCL, $C_{6–12}$) units. SCL PHAs, such as poly(3-hydroxybutyrate) [P(3HB)] and P(3HB-*co*-

3-hydroxyvalerate) are thermoplastics with stiff and brittle material properties. MCL PHA copolymers are low-crystalline polymer with ductile and many cases also sticky properties,[6] whereas MCL PHA homopolymers can be molded into a soft, transparent, and extensible film.[7,8] SCL-MCL random copolymers have intermediate properties of the aforementioned polymers, like moderate strength and flexibility, due to their reduced crystallinity. For example, poly[3HB-*co*-3-hydroxyhexanoate (3HHx)] is a random copolymer manufactured commercially for use in straws, plastic bags, etc.[9] To cover the wider range of applications, expansion of PHA properties is an important goal.

PHA synthase (PhaC) is a key enzyme that determines the monomeric composition of the polymers. PHA synthase are categorized into five groups based on their subunit structure and substrate specificity.[10,11] Class I PHA synthases are typically specific to SCL 3-hydroxyacyl (3HA)-coenzyme A (CoA), whereas class II enzymes recognize MCL 3HA monomers. The substrate specificity of other classes is similar to that of class I. Some PHA synthases, such as class I PhaC from *Aeromonas caviae* ($PhaC_{Ac}$)[10] and class II PhaC from *Pseudomonas* sp. 61-3 ($PhaC1_{Ps}$),[11] have broad substrate specificity and can incorporate both SCL and MCL 3HA monomers. These PhaCs are useful for producing SCL-MCL random copolymers.

Block copolymerization is an effective and versatile method for giving functional materials that cannot be achieved with homopolymers.[12] Biosynthesis of PHA block copolymers, therefore, has attracted research interest. In the early trials to synthesize PHA block copolymers, researchers attempted several strategies, like changing feedstock and/or monomer precursors during production.[13] In other words, different substrates for individual blocks are added using a sequential feeding mode. The sequence of the obtained polymers, however, needs further verification because

the time required to synthesize a single PHA molecule is thought to be much shorter than cultivation period;[14] thus, polymer blends rather than block copolymers could be synthesized.[15]

The discovery of sequence-regulating PHA synthase is a breakthrough in the biosynthesis of PHA block copolymers.[15] Sequence-regulating PHA synthase is capable of spontaneously synthesizing block copolymers from a mixture of monomer substrates without manipulations during polymer production. $PhaC_{AR}$, the first-discovered sequence-regulating PHA synthase, is a chimeric enzyme composed of N-terminal region of $PhaC_{Ac}$ and C-terminal region of PhaC from *Ralstonia eutropha* (*Cupriavidus necator*) ($PhaC_{Re}$).[16] It synthesizes poly(2-hydroxybutyrate)-*b*-poly(3-hydroxybutyrate) [P(2HB)-*b*-P(3HB)] in recombinant *E. coli* with supplementation of 2HB and 3HB.[15] $PhaC_{AR}$ is also characterized by the unusual substrate specificity toward 2HB-CoA. To date, only engineered PHA synthases incorporate 2HB units. The evolved class II enzyme $PhaC1_{Ps}$STQK is known to synthesize P(2HB).[17]

P(2HB)-*b*-P(3HB) is the first structure-verified PHA block copolymer. Its block sequence was verified by solvent fractionation and observation of microphase separation.[15] Recently, we reported that 2HB-rich P(2HB)-*b*-P(3HB) possesses elastomer-like properties,[18] a common characteristic of block copolymers.[19] In the copolymer, the combination of amorphous P(2HB) and crystalline P(3HB) phases, which served as soft and hard segments, respectively, contributed to the expression of elastomer-like properties. This finding indicates that PHA block copolymers may expand PHA mechanical properties. Useful and characteristic properties of block copolymers are attributable to the distinct properties of each segment. In this regard, PHA block copolymers composed of MCL and SCL segments are attractive targets. However, a major obstacle in molecular design is presented by $PhaC_{AR}$, which has a limited ability to incorporate MCL monomers.[18]

Here, we aimed to create engineered $PhaC_{AR}$ proteins with increased activity toward an MCL substrate, 3HHx. The goal was to biosynthesize a new type of PHA, an MCL-SCL block copolymer. Directed evolution is an effective approach to create engineered PHA synthases with desired function. Previous studies have demonstrated effective methodologies for random mutant library screening[20] and the rational protein structure design.[21,22] Here, we used random mutagenesis to explore the broad range of mutations. Candidates of beneficial PhaC mutants were selected using *in vivo* Nile Red plate assay.[20] This screening method is based on a positive correlation between cellular PHA content and fluorescent intensity of the colonies stained with a hydrophobic dye bound to the intracellularly accumulated PHA inclusion body.[23] Previously, the homopolymers of the target monomer have been chosen as an indicator polymer.[20] However, the method is not simply applicable to the present study because $PhaC_{AR}$ does not synthesize a homopolymer of the target monomer, P(3HHx). Thus, we designed a screening system that utilizes 3HHx-rich P(3HB-*co*-3HHx) as an indicator polymer. As a result, beneficial $PhaC_{AR}$ mutants with increased activity toward 3HHx-CoA were successfully obtained from the screening. Our results indicated that the $PhaC_{AR}$ mutant can synthesize a new MCL-SCL PHA block copolymer, P(3HHx)-*b*-P(2HB).

Experimental Section

Bacterial strains and plasmids. *E. coli* JM109 was the host for plasmid construction, screening, and polymer production. The plasmid $pBSP_{Re}phaC_{AR}pctalkK$ was used in this study.[24] This plasmid contains the chimeric PHA synthase gene (*phaC*$_{AR}$), propionyl-CoA transferase gene (PCT) from *Megasphaera elsdenii*, and the MCL 3-hydroxyalkanoic acid CoA ligase gene (*alkK*) from *Pseudomonas putida*[22] under the control of the *phb* operon promoter P_{Re} from *R. eutropha*.[15] The *phaC*$_{Re}$ region in *phaC*$_{AR}$ was replaced with the codon-optimized fragment for expression in *E. coli*,

which was synthesized by Eurofins Scientific (Luxembourg). The modified plasmid is referred to as $pBSP_{Re}phaC_{AR}$(opt)pctalkK, and its sequence is shown in Supplementary Information (Appendix 1). Unless mentioned otherwise, all chemicals were purchased from Tokyo Chemical Industry (Japan), Bio-Rad Laboratories (USA), JUNSEI Chemical (Japan), or FUJIFILM Wako Pure Chemicals Corporation (Japan).

Random mutagenesis of $phaC_{AR}$ by error-prone PCR. Random mutagenesis was performed on the $phaC_{Ac}$ and the $phaC_{Re}$ regions of the $phaC_{AR}$ gene. The following pairs of primers were used: 5′-CGGCCGACCTCAAACGCGCTCTCGTC-3′; 5′-TGACTCGAGCCGGTTCGAATCTAGA-3′ for the $phaC_{Ac}$ region and 5′-ATGATGGAAGACCTGACACG-3′; 5′-GCGCATTGCCATAGTTGG-3′ for the $phaC_{Re}$ region, respectively. The error-prone PCR mixture contained 100 $ng \cdot \mu L^{-1}$ $pBSP_{Re}phaC_{AR}$pctalkK or $pBSP_{Re}phaC_{AR}$(opt)pctalkK as the templates, 10 μM primers, 0.2 mM dNTPs, 0.025 mM $MnCl_2$, 1.5 mM $MgCl_2$,[25] 10 mM Tris-HCl (pH 8.8), and 50 mM KCl. H_2O was removed from this mixture by freezing-dry and replaced by D_2O. 0.05 U r*Taq* DNA polymerase was added into the mixture. For the $phaC_{Ac}$ region, the amplified fragment was digested with *Bgl*II and *Xba*I and inserted into $pBSP_{Re}phaC_{AR}$pctalkK digested by the same enzymes for substituting the corresponding region. For the $phaC_{Re}$ region, the amplified fragment was inserted into $pBSP_{Re}phaC_{AR}$(opt)pctalkK in a similar manner using *Bgl*II and *Sfi*I.

Construction of a site-directed saturation mutagenesis library. Site-directed saturation mutagenesis at position 314 was performed by overlap extension PCR using $pBSP_{Re}phaC_{AR}$(opt)pctalkK as the template and following primers: F1: 5′-AACTTCCTTGCCACCAATCC-3′; R1: 5′-TCATGCCTTGGCTTTGAC-3′; F314X_F: 5′-CGGTCAGGATAAAATCAATGTTCTGGGTNNNTGTGTTGGTGGC-3′; F314X_R: 5′-

ACCCAGAACATTGATTTTATCCTGACCG-3′. Underlined bases correspond to the 314th amino acid residue replaced by the following codons individually to introduce site-directed saturation mutagenesis; A (GCG), C (TGC), D (GAT), E (GAA), F (TTT), G (GGC), H (CAT), I (ATT), K (AAA), L (CTT), M (ATG), N (AAC), P (CCG), Q (CAG), R (CGC), S (AGC), T (ACC), V (GTG), W (TGG), and Y (TAT). Mutated fragments and pBSP$_{Re}$phaC$_{AR}$(opt)pctalkK were digested with *Bgl*II and *Sfi*I before ligation to obtain a mutant library.

Culture conditions. To select the beneficial mutant candidates of *phaC$_{AR}$*, the mutant gene library was introduced into *E. coli* JM109. Cells were grown on agar plates of Luria–Bertani (LB) medium containing 5 g·L^{-1} yeast extract, 10 g·L^{-1} tryptone, 10 g·L^{-1} NaCl, 2 wt% glucose, 0.5 mg·L^{-1} Nile Red, 100 mg·L^{-1} ampicillin, 1.0 g·L^{-1} sodium (*R,S*)-3-hydroxybutyrate (3HB-Na), 2.5 g·L^{-1} sodium (*R,S*)-3-hydroxyhexanoate (3HHx-Na), and 15 g·L^{-1} agar. Beneficial mutant candidates were selected on the basis of the fluorescent intensity of colonies.[26] 3HHx-Na was prepared from ethyl 3HHx as previously reported.[27]

P(3HB-*co*-3HHx) production by the selected mutant candidates was investigated using the liquid medium with the same composition (without Nile Red and agar). P(3HB) and P(3HHx) were also produced with the supplementation of 3HB-Na and 3HHx-Na as sole precursors, respectively. *E. coli* JM109 harboring pBSP$_{Re}$PhaC$_{AR}$pctalkK, pBSP$_{Re}$PhaC$_{AR}$(opt)pctalkK, or their mutated derivatives were cultivated in 1.5 mL medium in a test tube at 30 °C for 48 h. Polymer production and monomer composition were determined via gas chromatography (GC) as described previously.[28] For nuclear magnetic resonance (NMR) analysis of P(3HB-*co*-3HHx), the cells were cultured in 100 mL medium containing 2.5 g·L^{-1} 3HB-Na and 1.0 g·L^{-1} 3HHx-Na in 500-mL shake flasks with reciprocal shaking at 120 rpm at 30 °C for 48 h. Polymers were extracted with chloroform at 60°C for 48 h and purified via polymer precipitation by adding excess methanol.

The purification step was repeated twice. ^{13}C NMR of the extracted polymer was analyzed in $CDCl_3$ as described previously.[29]

For producing P(2HB), P(3HHx), and P(2HB-*co*-3HHx) at the flask scale, the cells harboring pBSP$_{Re}$PhaC$_{AR}$(opt)pctalkK or its derivative were cultivated in 100 mL medium containing 2.5 g·L^{-1} sodium (*R*,*S*)-2-hydroxybutyrate (2HB-Na) and/or 1.0 g·L^{-1} 3HHx-Na in 500-mL shake flasks with reciprocal shaking at 120 rpm at 30 °C for 50 h. The precursors were added at 2 h after inoculation. Polymers were extracted as described above. Polymer production was determined by weight. Monomer composition was determined using ^{1}H NMR.

Immunoblot analysis. Cells harboring pBSP$_{Re}$PhaC$_{AR}$(opt)pctalkK and its derivative were cultivated in 1.5 mL LB medium containing 100 mg·L^{-1} ampicillin at 30 °C for 14 h and harvested via centrifugation (15,300 *g*, 3 min, 4 °C). The cells were resuspended in 0.2 mL 20 mM lysis buffer (pH 7.5)[30] and disrupted by sonication on ice for 10 min. After centrifugation (15,300 *g*, 3 min, 4 °C), the obtained supernatant was referred to as crude extract. Crude extract protein concentration was determined using Bradford assay.[31] Immunoblot analysis was performed following reported methodology using anti-PhaC$_{Re}$ antibody as the primary antibody.[32]

Preparation of CoA thioesters and enzyme activity assay. (*R*,*S*)-3-Hydroxybutyryl-CoA (3HB-CoA) was synthesized from (*R*,*S*)-3-hydroxybutyric acid. The CoA thioesters were prepared using a modified method[33] as follows: 1,1′-carbonyldiimidazole (42.2 mg) was dissolved in 2 mL dry tetrahydrofuran (THF). (*R*,*S*)-3-Hydroxybutyric acid (109 mg) was then added, and the mixture was incubated for 30 min with stirring at room temperature (~25 °C). CoA (40 mg) (Oriental Yeast, Tokyo, Japan) was dissolved in 1 mL of 0.5 M $NaHCO_3$ (pH 7.4), and the solution was combined with the THF solution and incubated for 12 h with stirring on ice. The reaction mixture was diluted with 9 mL of 0.5 M $NaHCO_3$. After acidification using formic acid to pH ~ 3, THF was evaporated

in vacuo. 3HB-CoA was purified using a preparative high-performance liquid chromatography (HPLC) equipped with a reverse-phase column (ODS-80Ts, TOSOH, Japan) using 5 mM ammonium acetate (pH 5.5) and acetonitrile as mobile phases. The fractions containing 3HB-CoA were collected, and acetonitrile was evaporated *in vacuo*. The synthesis of 3HB-CoA was confirmed by LC-electrospray ionization-mass spectroscopy (LC-ESI-MS) (LCMS2020, Shimadzu, Japan). The concentration of 3HB-CoA was determined by the absorbance at 259 nm using a molar attenuation coefficient of 1.64×10^4 M^{-1} cm^{-1}. (*R,S*)-3-Hydroxyhexanoyl-CoA (3HHx-CoA) was synthesized in the same manner using 162 mg 3HHx-Na.

An *in vitro* enzyme activity assay was conducted using crude extract and CoA thioesters prepared as described above. For 3HB-CoA, the reaction mixture (62 μL) contained 65 ng·μL^{-1} crude extract, 2.1 mM 3HB-CoA, and 1.1 μg·μL^{-1} bovine serum albumin (BSA) in 40 mM potassium phosphate buffer (pH 7.4). For 3HHx-CoA, the reaction mixture (75 μL) contained 400 ng·μL^{-1} crude extract, 1.7 mM 3HHx-CoA, and 0.9 μg·μL^{-1} BSA in the same buffer. The reaction was performed in a 96-well microplate. After addition of crude extract to initiate the reaction, 60 μL 1% trichloroacetic acid was periodically added for quenching. The reaction solution was filtered via centrifugation (12,000 *g*, 10 min, 4 °C) using filtering microplates with 0.45 μm pore size (Cytiva, USA). An aliquot of 100 μL filtrate was transferred to a new microplate and 60 mL of 1 mM 5,5′-dithiobis(2-nitrobenzoic acid) (DTNB) (Merck, Germany) was added. Released free CoA was quantified by measuring absorbance at 412 nm. One unit of enzyme activity is defined as the amount required to catalyze the transformation of 1 μmol substrate in 1 min.[34]

Solvent fractionation of polymers. To distinguish block copolymer from polymer blend, purified polymer samples were fractionated into two fractions depending on their solubility in organic solvents.[35,36] Approximately 8 mg of purified polymer sample was dissolved in 0.5 mL THF in a

test tube with a screw cap by heating at 60 °C for 10 min. After cooling down to room temperature, the solution was combined with 6 mL cyclohexane and incubated at 18 °C for 1 h. The precipitant collected on a PTFE filter membrane (pore size 0.1 μm) is referred to as the insoluble fraction. The flow-through fraction is referred to as the soluble fraction. The components in both insoluble and soluble fractions were recovered in $CDCl_3$ and analyzed using ^1H NMR. The same experiment was conducted using a polymer blend composed of two homopolymers P(2HB) and P(3HHx).

Protein structure prediction. Five structural models of $PhaC_{AR}$ were predicted using the Google collaborative notebook for AlphaFold2 prediction (https://colab.research.google.com/github/sokrypton/ColabFold/blob/main/AlphaFold2.ipynb). Model 1 is used for interpretation because it had the highest confidence score. The per-residue confidence score provided by AlphaFold2 (named pLDDT[1]) was above 80% for 85% of the residues. The hydrophobicity of the residues was calculated based on the hydrophobicity scale defined by Eisenberg et al.[37]

Results

Exploration of beneficial mutations in the $PhaC_{Ac}$ region. The metabolic pathway used in this study is shown in Figure 1. P(3HB-*co*-3HHx) was used as an indicator polymer because $PhaC_{AR}$ does not synthesize P(3HHx) homopolymer. The copolymer possesses a random sequence based on ^{13}C NMR (Figure S1). Supplementation of 1.0 $g \cdot L^{-1}$ 3HB-Na and 2.5 $g \cdot L^{-1}$ 3HHx-Na enabled the synthesis of P(3HB-*co*-3HHx) with approximately 50 mol% 3HHx (Table 1). This synthesis of the 3HHx-rich P(3HB-*co*-3HHx) allowed us to isolate candidates having enhanced capacity to incorporate 3HHx units.

First, the random mutant library of the N-terminal region of the *phaC*$_{AR}$ (the *phaC*$_{Ac}$ region) was subjected to screening. *E. coli* expressing the enzymes in the metabolic pathway in Figure 1 was grown on Nile red plates. Six colonies with stronger fluorescence, which can be expected to produce greater amount of 3HHx-rich P(3HB-*co*-3HHx) were selected from approximately 1,000 colonies. The selected *phaC*$_{AR}$ mutants contained either N149D or H121Y mutation. The liquid culture using the isolated mutants indicated that N149D was particularly effective at enhancing 3HHx incorporation (Table 1).

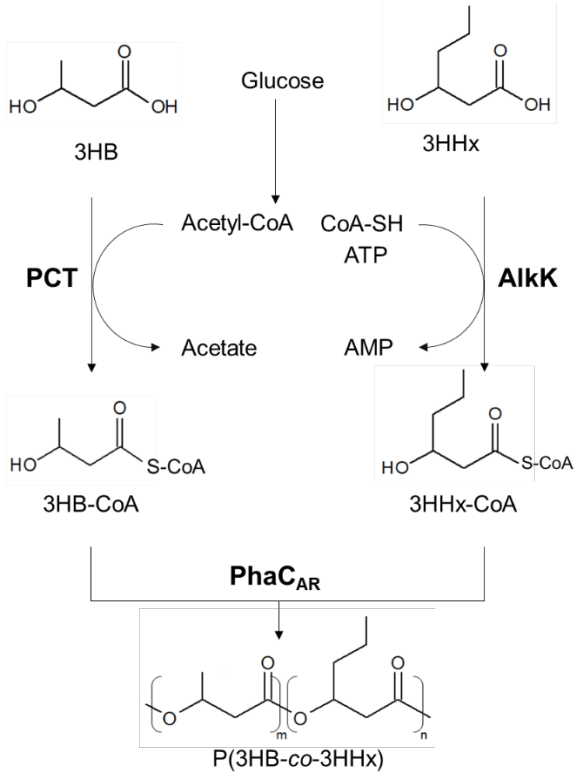

Figure 1. Metabolic pathway used in the study. The monomer precursors, 3HB and 3HHx, are supplemented into the medium. PCT and AlkK serve as monomer supplying routes for 3HB-CoA and 3HHx-CoA, respectively.

Table 1. The effects of mutations in the PhaC$_{Ac}$ region in PhaC$_{AR}$ on the production of P(3HB-*co*-3HHx).

$PhaC_{AR}$ mutants	Cell dry weight ($g \cdot L^{-1}$)	Polymer content (wt%)	Monomer composition (mol%)	
			3HB	3HHx
Parent	1.5 ± 0.0	22.5 ± 2.4	47.6 ± 0.7	52.4 ± 0.7
H121Y	1.5 ± 0.2	26.1 ± 1.6	43.6 ± 0.4	56.4 ± 0.4
N149D	1.5 ± 0.1	36.6 ± 3.3	37.9 ± 1.5	62.1 ± 1.5

Note: Cells harboring $pBSP_{Re}phaC_{AR}$pctalkK and its derivatives were used for polymer production. Data are presented as mean ± standard deviation of the biological triplicate.

Exploration of beneficial mutations in the $PhaC_{Re}$ region. Next, the random mutant library of the C-terminal region of *phaC*$_{AR}$ (the *phaC*$_{Re}$ region) was screened. Error-prone PCR amplification of the region was unsuccessful, presumably due to its high G/C content (67%). Codon usage in the *phaC*$_{Re}$ region was therefore optimized for expression in *E. coli*, and the G/C content was reduced to 50%. From approximately 2,000 colonies, three candidates (T319I, V454D/I509V, and F314L) exhibiting strong fluorescence were isolated. These mutants were tested for polymer production via liquid culture. The selected mutations increased PHA production, 3HHx fraction, or both (Table 2). Among the analyzed mutants, F314L exhibited the highest 3HHx fraction (62.6 mol%), suggesting that the position plays an important role in substrate recognition. Indeed, this residue is adjacent to the catalytic center residue Cys315, which corresponds to Cys319 in $PhaC_{Re}$. On the basis of these results, the mutation at position 314 was subjected to further investigation.

Table 2. The effects of mutations in the $PhaC_{Re}$ region in $PhaC_{AR}$ on the production of P(3HB-*co*-3HHx).

$PhaC_{AR}$ mutants	Cell dry weight ($g \cdot L^{-1}$)	Polymer content (wt%)	Monomer composition (mol%)

			3HB	3HHx
Parent	1.9 ± 0.1	46.2 ± 1.4	58.4 ± 0.9	41.6 ± 0.9
F314L	2.6 ± 0.1	49.7 ± 0.9	37.4 ± 0.7	62.6 ± 0.7
T319I	2.2 ± 0.0	44.1 ± 2.3	49.4 ± 1.4	50.6 ± 1.4
V454D/ I509V	2.2 ± 0.1	53.6 ± 1.0	47.1 ± 0.2	52.9 ± 0.2

Note: Cells harboring pBSP$_{Re}$phaC$_{AR}$(opt)pctalkK and its derivatives were used for polymer production. Data are presented as mean ± standard deviation of the biological triplicate.

Saturation mutagenesis at position 314. Site-directed saturation mutagenesis at position 314 was conducted. The 19 mutant genes and the parent *phaC*$_{AR}$ gene were individually expressed in *E. coli* to test their capacity to produce P(3HB-*co*-3HHx) (Figure 2A). As a result, various functional groups were acceptable at this position. F314H, F314L, F314M, and F314Q exhibited particularly high (1.4 to 1.5-fold) polymer production compared with the parent PhaC$_{AR}$. Substitutions with K, N, P, and R, however, considerably decreased polymer production. Surprisingly, all mutants exhibited a higher 3HHx fraction than the parent enzyme. In addition, many of the mutants displayed 1.4 to 2.0-fold higher accumulation of 3HHx units than the parent enzyme. In contrast, most mutants produced a reduced amount of P(3HB) homopolymer (Figure 2B). These results suggest that the residue at position 314 contributes to substrate specificity of the enzyme.

Parent PhaC$_{AR}$ is incapable of synthesizing P(3HHx) homopolymer in *E. coli*. The enhanced 3HHx incorporation capacity of the isolated mutants motivated us to test their ability to synthesize P(3HHx). *E. coli* individually expressing the saturation mutants was cultivated with supplementation of 3HHx as a sole precursor. As a result, many mutants produced P(3HHx) homopolymer (Figure 2C). The P(3HHx) production was comparable (approximately 0.6-fold) with that of P(3HB).

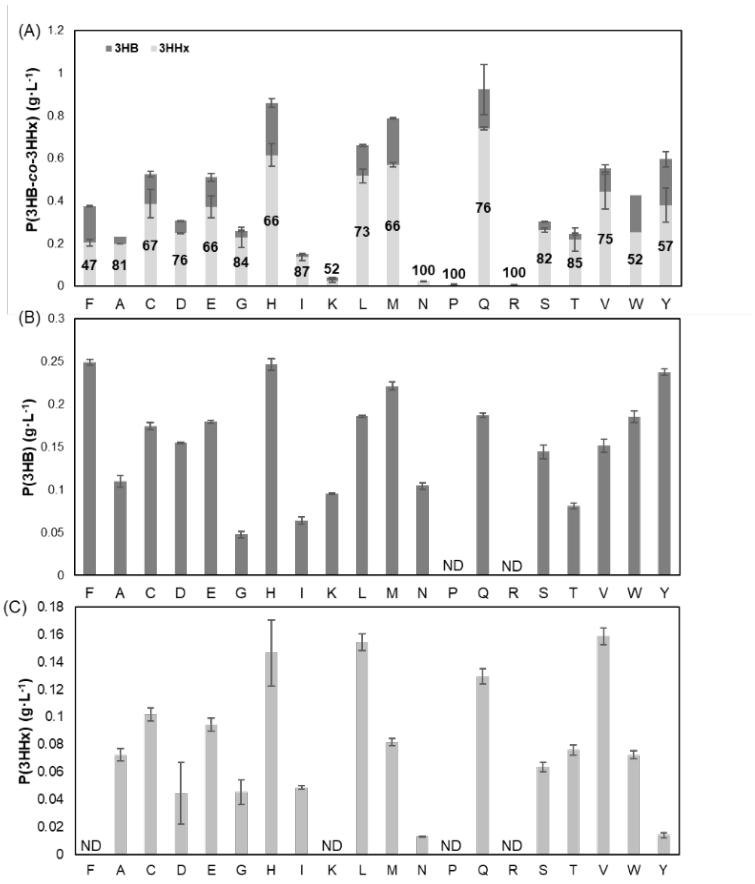

Figure 2. Copolymer and homopolymers production by saturation mutants at position 314. X-axis indicates amino acid residues at position 314 (F is the parent enzyme), and Y-axis indicates polymer production. (A) P(3HB-*co*-3HHx) copolymer production, (B) P(3HB) homopolymer production, and (C) P(3HHx) homopolymer production. Dark gray bar, 3HB; and light gray bar, 3HHx. The numbers at the center of the gray bars in panel (A) indicate the 3HHx fraction (mol%). Data are presented as mean ± standard deviation of the biological triplicate. ND, not detected.

Immunoblotting analysis. To examine expression levels of the $PhaC_{AR}$ F314X mutants, immunoblot analysis was conducted using the crude cell extracts and the anti-$PhaC_{Re}$ antibody (Figure 3). The expression levels of F314P and F314R significantly decreased, which accounted for the low polymer production of these mutants (Figure 2). For the other mutants, expression

levels were comparable or slightly lower than that of the parental enzyme. These results demonstrated that the enhanced incorporation of 3HHx units by mutated $PhaC_{AR}$ was likely due to their increased activity toward 3HHx-CoA rather than elevated expression levels of the protein.

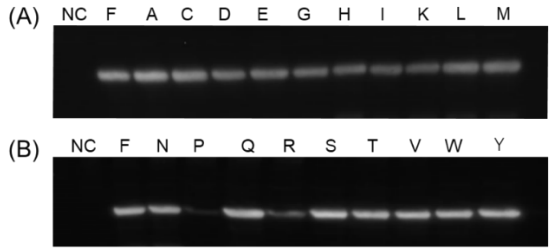

Figure 3. Immunoblot analysis of saturation mutations at position 314 in $PhaC_{AR}$ using crude cell extracts and the anti-$PhaC_{Re}$ antibody. NC, negative control (the crude extract of *E. coli* harboring the empty plasmid, pUC18); single letters indicate the F314X substitutions. The full membrane image is shown in Supporting Information Figure S2.

Enzyme activity assay. Enzyme activity and substrate specificity were evaluated via *in vitro* analysis. The F314H mutant was chosen because of its high P(3HHx) and P(3HB) production capacity (Figure 2). We found that both the parent and F314H enzymes exhibited clear consumption of 3HB-CoA (Figure 4A). The activity of the parent enzyme to 3HB-CoA was 2.4-fold higher than that of F314H (Figure 4C). In contrast, the parent enzyme exhibited very small consumption of 3HHx-CoA, whereas F314H exhibited remarkable activity (Figure 4B). The immunoblot analysis indicated that the expression levels of these enzymes were comparable (Figure 3). On the basis of this result, we determined that F314H possesses shifted substrate specificity toward 3HHx-CoA (Figure 4C) consistent with the *in vivo* polymer production result.

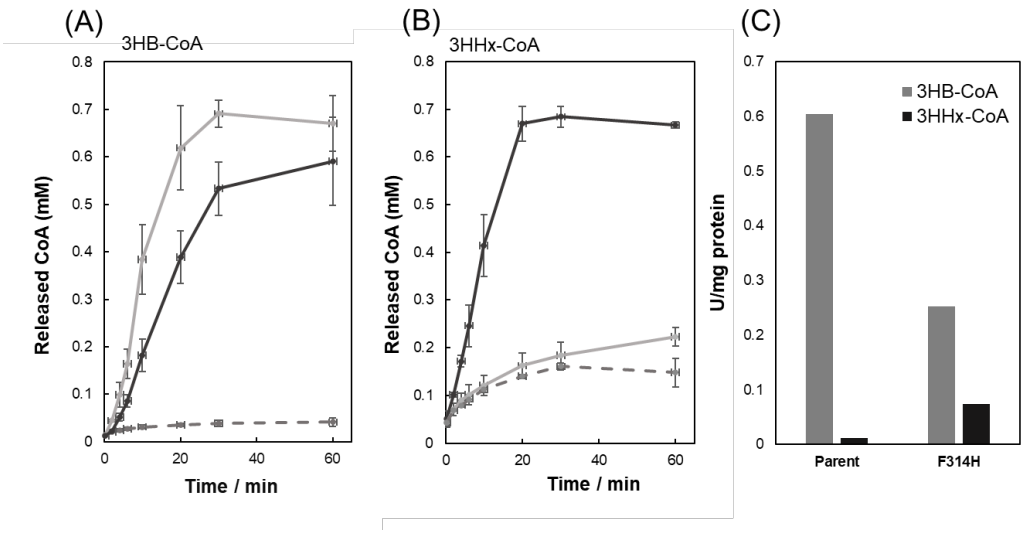

Figure 4. *In vitro* enzymatic activity analysis of the parent and F314H mutant of $PhaC_{AR}$. The CoA release from 3HB-CoA (A); the CoA release from 3HHx-CoA (B); and the enzymatic activity toward 3HB-CoA (gray bar) and 3HHx-CoA (black bar) (C). Enzyme activity was calculated using initial velocities. Gray lines, parent; black lines, F314H; and dashed lines, negative control (empty pUC18).

Monomer sequence analysis of copolymers synthesized by $PhaC_{AR}$F314H. The directed evolution of $PhaC_{AR}$ successfully created beneficial mutants with reinforced activity toward 3HHx-CoA. Among them, $PhaC_{AR}$F314H was used for the monomer sequence analysis of the polymers.

The monomer sequence of P(3HB-*co*-3HHx) synthesized by $PhaC_{AR}$F314H was determined by ^{13}C NMR analysis (Figure 5A). The signals corresponding to the carbonyl group of 3HB and 3HHx were observed at δ 169–170. These signals were ascribed to the dyad sequences of 3HB*-3HB, 3HB*-3HHx or 3HHx*-3HB, and 3HHx*-3HHx.[38] An abundance of 3HB-3HHx/3HHx-3HB dyads indicates that the P(3HB-*co*-3HHx) synthesized by $PhaC_{AR}$F314H has a random sequence. In addition, we calculated D value, which is an index of monomer sequence.[39] The D value of the

produced P(3HB-*co*-3HHx) was 4.6 (Supporting Information Appendix 2), also suggesting a random sequence.

Previously, it was reported that the presence of 2HB monomer is a key for block copolymer synthesis using the sequence-regulating PHA synthase, $PhaC_{AR}$. The capacity of $PhaC_{AR}$F314H to synthesize P(3HHx) homopolymer prompted us to synthesize the copolymers of 3HHx and 2HB (Table 3). P(2HB) synthesis was also attempted as a control. In this experiment, the monomer precursors were added at 2 h after inoculation, which facilitates the cell growth.

The F314H mutant was capable of synthesizing P(2HB), P(3HHx), and the binary polymer (Table 3). Notably, this is the first report of P(2HB) and P(3HHx) syntheses by class I PHA synthase. It has been known that synthesis by class I PHA synthase creates higher molecular weight polymer than that by class II PHA synthase. In fact, the molecular weight of the obtained homopolymers (Table 3) was one order of magnitude higher than that of P(2HB) ($M_w = 2.7 \times 10^4$)[17] and P(3HHx) ($M_w = 2.7 \times 10^5$)[40] obtained by class II PHA synthase. In addition, ^{1}H NMR of the obtained binary polymer indicated that the resonance of methine proton of 2HB units, which is a fingerprint region to judge triad sequences, was observed at single chemical shift corresponding to a 2HB-2HB*-2HB triad (Figure 5B). No detection of 3HB-2HB sequence indicates that there is long region(s) containing successive 2HB units. These results indicate the presence of the P(2HB) homopolymer structure in the polymer. The obtained binary polymer is therefore either a block copolymer or a blend of the two homopolymers P(3HHx) and P(2HB). In contrast, the parent $PhaC_{AR}$ did not synthesize polymers under these conditions.

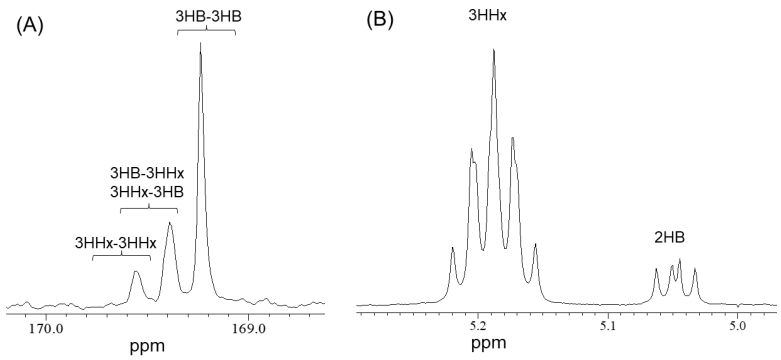

Figure 5. ^{13}C NMR of carbonyl carbons in P(3HB-*co*-3HHx) (A) and ^{1}H NMR of methine protons in binary polymer containing 3HHx and 2HB (B). The polymers in (A) and (B) were obtained by using PhaC$_{AR}$F314H. Full spectra are shown in Figures S3 and S4, respectively.

Table 3. P(2HB), P(3HHx), and binary polymer synthesis by PhaC$_{AR}$F314H mutant

PhaC$_{AR}$	Monomer precursor concentration (g·L^{-1})		Cell dry weight (g·L^{-1})	Polymer production (mg·L^{-1})	Monomer composition (mol%)		Molecular weight		
	3HHx	2HB			3HHx	2HB	M_n (× 10^5)	M_w (× 10^5)	M_w/M_n
Parent	1.0	0	1.8 ± 0.0	ND	ND	-			
Parent	0	2.5	2.7 ± 0.0	ND	-	ND			
Parent	1.0	2.5	0.5 ± 0.0	trace	ND	ND			
F314H	1.0	0	2.5 ± 0.1	115 ± 13	100	0	3.4	11.6	3.4
F314H	0	2.5	2.9 ± 0.1	59 ± 8	0	100	1.5	4.2	2.9
F314H	1.0	2.5	2.8 ± 0.1	122 ± 8	93	7	4.0	11.1	2.8

Note: Cells harboring pBSP$_{Re}$phaC$_{AR}$(opt)pctalkK (parent) and pBSP$_{Re}$phaC$_{AR}$(opt)F314HpctalkK (F314H) were used for polymer production. Cells were cultivated for 50 h. Precursors were added at 2 h after inoculation. Data are presented as mean ± standard deviation of the biological triplicate. ND, not detected.

Solvent fractionation. Solvent fractionation was performed to determine the presence or absence of a covalent linkage between P(3HHx) and P(2HB) segments in the binary polymer. The solubility test found that cyclohexane moderately dissolves P(3HHx) but not P(2HB). This distinct solubility in cyclohexane was utilized for the solvent fractionation. The blend of P(3HHx) and P(2HB) was dissolved in THF and precipitated by adding cyclohexane. As expected, the cyclohexane-soluble fraction did not contain P(2HB) (Table 4). Detection of P(3HHx) in the cyclohexane-insoluble fraction may be due to co-precipitation with P(2HB). Next, the binary polymer synthesized by the F314H mutant was subjected to the same procedure. As a result, P(2HB) was detected not only in the cyclohexane-insoluble fraction but also in the cyclohexane-soluble fraction (Figure S5). This result strongly indicates the presence of covalent linkage between P(3HHx) and P(2HB) segments. Based on these results, we concluded that the obtained polymer was a block copolymer P(3HHx)-*b*-P(2HB).

Table 4. Solvent fractionation of P(3HHx-*co*-2HB) synthesized by $PhaC_{AR}F314H$

Polymers[a]	Monomer composition (mol%)		Recovery (mol%)
	3HHx	2HB	
P(3HHx)	100	0	100
Soluble fraction	100	0	86
Insoluble fraction	-	-	trace
P(2HB)	0	100	100
Soluble fraction	-	-	trace
Insoluble fraction	0	100	90
Blend of P(3HHx) and P(2HB) (94:6 mixture)	94	6	100

Soluble fraction	100	0	29
Insoluble fraction	94	6	67
Original Copolymer	93	7	100
Soluble fraction	96	4	50
Insoluble fraction	91	9	48

Note: [a] The homopolymers and copolymers were synthesized using the conditions described in Table 3. The recovery ratio was calculated on the basis of the molar ratio of 3HHx and 2HB in each soluble and insoluble fraction compared with the original copolymer (before fractionation). The molar ratio of 3HHx and 2HB in copolymer was measured using ^{1}H NMR.

Discussion

This study describes the biosynthesis of the first MCL-SCL block copolymer, which was achieved by evolving the sequence-regulating PHA synthase. Conventional strategies for regulating physical properties of PHAs are based on reducing crystallinity by random copolymerization, which contributes to soft and pliable properties. Block copolymers can exert characteristic properties due to their microphase separation structure. For that, the combination of segments with distinct properties is preferable. The new component MCL homopolymer facilitates the molecular design of PHA block copolymers that combines soft and hard segments. MCL-SCL block copolymerization, therefore, provides an effective strategy for regulating PHA physical properties. The thermal and mechanical properties of P(3HHx)-*b*-P(2HB) will be reported in our future work.

Acquiring the P(3HHx)-synthesizing capacity was key to enabling MCL-SCL block copolymer synthesis, because the parental $PhaC_{AR}$ synthesizes no P(3HHx). The inability of homopolymer synthesis is also observed in other PHA synthases. For example, $PhaC1_{Ps}$ from *Pseudomonas* sp. 61-3 synthesized a tiny amount of P(3HB) (< 0.1 wt%) in *E. coli*,[41] whereas the enzyme synthesized P(92 mol% 3HB-*co*-MCL 3HA) with a polymer content of 45 wt% in *Pseudomonas* sp. 61-3.[42]

Such incapability (or very low efficiency) of homopolymer synthesis is presumably due to the potential barrier to initiate the polymerization, which is observed as a slow reaction at the initial stage of the reaction. This stage is referred to as the lag phase. Some unpreferred monomer substrates may not overcome the barrier; thus, their homopolymers are not synthesized efficiently. The results of the present study demonstrate that the homopolymer-synthesizing capacity can be acquired by evolving PHA synthase. Similarly, PhaC1$_{Ps}$STQK, which is a derivative of PhaC1$_{Ps}$, synthesizes P(3HB) with content comparable with that of PhaC$_{Re}$.[34]

For the directed evolution of PhaC$_{AR}$, mutations were introduced into the entire sequence of the enzyme. The beneficial mutation sites were found in N- and C-terminal regions, suggesting that mutagenesis and screening were performed in an unbiased manner. In particular, the mutations at position 314 in PhaC$_{AR}$ effectively increased activity toward 3HHx-CoA. Position 314, which is adjacent to the catalytic center cysteine residue C315, likely contributes to interaction with substrates. The mutation at the corresponding position in PhaC$_{Ac}$, which was selected by a rational design based on enzyme structure, was recently reported to slightly increase the 3HHx fraction.[43] The distinct mutation effect in PhaC$_{AR}$ and PhaC$_{Ac}$ suggests that the slight structural difference of the substrate binding pocket could drastically influence the mutation effect. These results demonstrate the effectiveness of the function-based screening employed here. In addition, it should be noted that the parent enzyme (F314) exhibited the lowest 3HHx fraction in P(3HB-*co*-3HHx) among the F314X saturation mutants (Figure 2). Contrarily, the parent enzyme accumulated the highest amount of P(3HB) among them. These results clearly indicate that F314 is favored in the natural selection for producing P(3HB) rather than a 3HHx-containing copolymer. This interpretation correlates with the specific and high activity of PhaC$_{Re}$ toward 3HB-CoA.[44]

The N149D mutation is located near the junction site of $PhaC_{Ac}$ and $PhaC_{Re}$ regions. N149 in $PhaC_{AR}$ corresponds to D153 in $PhaC_{Re}$ based on the amino acid alignment. D153 in $PhaC_{Re}$ is highly conserved in other $PhaC_{Re}$ homologs, suggesting that the residue has an important role. In addition, the position of N149D mutation is the same as the beneficial mutation N149S found in $PhaC_{Ac}$, which was chosen on the basis of P(3HB) production as a selection criterion.[41] The selection of the same position from $PhaC_{AR}$ and $PhaC_{Ac}$ suggests that the N-terminal region including this position is responsible for independent function of the enzyme. These facts caused our interest in the function and structure of the N-terminal region. Currently, interpreting the effect of mutation in the N-terminal region based on the 3-D structure is difficult because the full-length structure of PHA synthase has not been analyzed. To overcome this limitation, the protein structure prediction of $PhaC_{AR}$ was performed using AlphaFold2, which can calculate highly confident structures without using homolog structures.[45] The major part of the enzyme structure was predicted with a high confidence score (Figure 6). The high confidence score of the C-terminal $PhaC_{Re}$ region (> 90% confidence score in most residues) is due to the availability of the crystal structure of the catalytic domain (Figure 6A).[46] The structure of the approximately 50 N-terminal residues is not reliable because of a low confidence score.

The predicted full-length structure showed that $PhaC_{AR}$ is composed of mainly two domains (referred as N- and C-terminal domains) (Figure 6A). It should be noted that the boundary of the domains does not correspond to the junction site between $PhaC_{Ac}$ and $PhaC_{Re}$ regions. The N-terminal domain mostly corresponds to the N-terminal region in the primary structure of the enzyme, and vice versa. An exception is the region of 383-408th residues [designated as the cross-domain (CD) region] containing two α-helices, which are parts of the C-terminal $PhaC_{Re}$ region but included in the N-terminal domain. The CD region is included in the previously proposed LID

region, which was hypothesized to be opened so that the enzyme could accept the substrate.[47,48] In fact, the predicted structure indicates the opened conformation of the region. N149 in $PhaC_{AR}$ is located close to the CD region (presumably interacting with N396). Interestingly, a similar structure is found in the predicted structure of class II $PhaC1_{Ps}$ (Figure 6B), which also possesses a CD region (359-385th residues). The E130 residue is located close to the CD region (presumably interacting with N372). The amino acid sequences of the CD regions in $PhaC_{AR}$ and $PhaC1_{Ps}$ have 24/26 identity, indicating an important and common role of this region. Indeed, the E130D mutation in $PhaC1_{Ps}$ is known to increase activity toward 3HB-CoA.[27] The predictions suggest, therefore, that there is a common mechanism for the mutation effect between N149D in $PhaC_{AR}$ (as well as N149S in $PhaC_{Ac}$) and E130D in $PhaC1_{Ps}$.

The predicted structure of $PhaC_{AR}$ enables to estimate its surface hydrophobicity (Figure S6). The hydrophobicity map indicates the presence of a highly hydrophobic surface in the N-terminal domain, which could contribute to dimerization of the protein, association with PHA inclusions, or both. In fact, the N-terminal region was proposed to be important for dimerization.[47,49] Substitutions of the N-terminal hydrophobic residues with hydrophilic residues abolished PHA synthesis,[50] indicating that the hydrophobic region is essential for PhaC activity. In addition, there are two tunnels in the predicted structure (Figure S6). The catalytic cysteine Cys315 is located at the end of the tunnels, and one of the two tunnels is connected to the N-terminal hydrophobic surface, suggesting that the tunnels could be an entrance of monomers and an exit of synthesized PHA chains. The interpretation is consistent with the previous proposal that N-terminal domain binds to the nascent PHA chains.[46]

The synthesis of a block copolymer by using F314H mutant indicates that sequence-regulating capacity of $PhaC_{AR}$ was maintained despite broadening its substrate specificity. Currently, the

mechanism for the generation of block sequence is not fully understood. In the case of P(2HB)-*b*-P(3HB), contrasting activity of $PhaC_{AR}$ toward 2HB-CoA and 3HB-CoA partly accounts for the block copolymerization.[15] Detailed in vitro analysis using 3HHx-CoA is needed to clarify the problem.

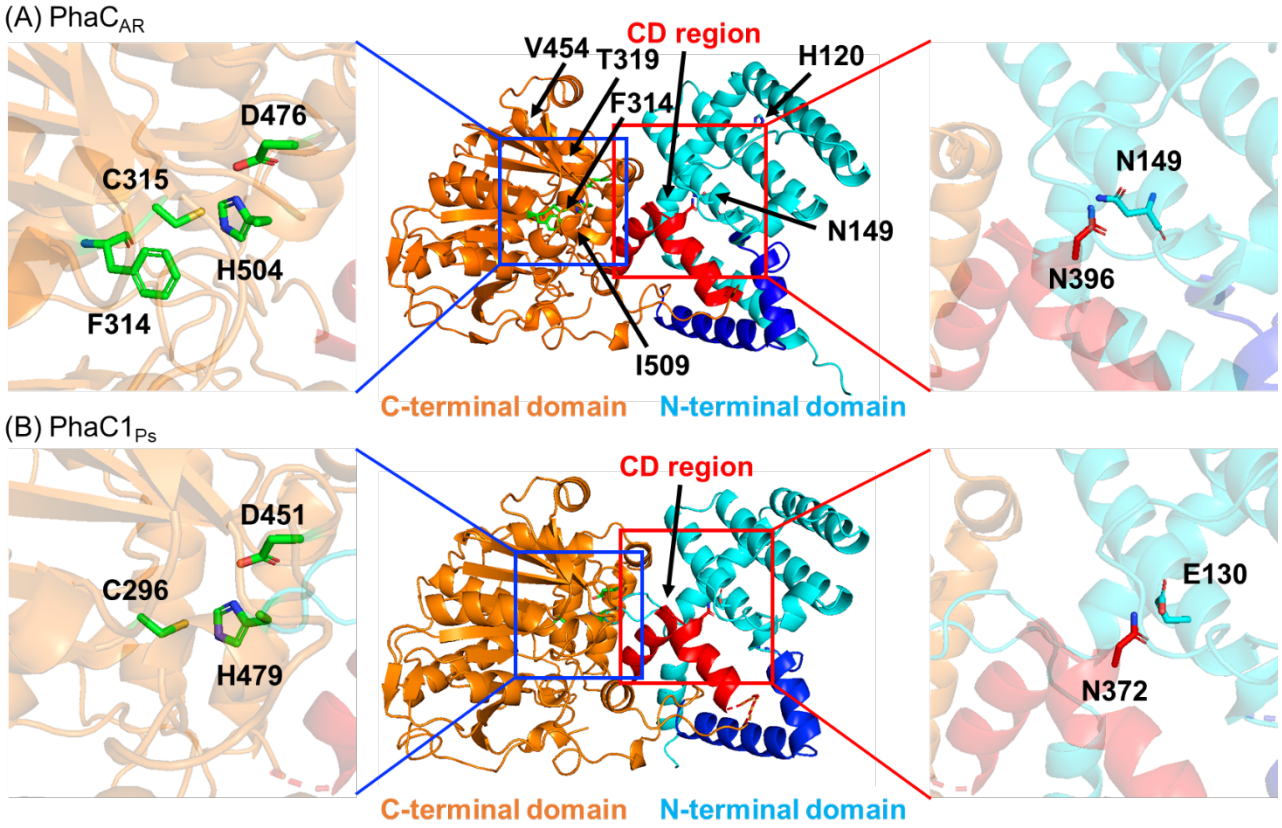

Figure 6. Predicted tertiary structures of $PhaC_{AR}$ and $PhaC1_{Ps}$. Overall structures of $PhaC_{AR}$ (A). Cyan, $PhaC_{Ac}$ region (N-terminal domain); dark blue, part of $PhaC_{Re}$ region (N-terminal domain); orange, part of $PhaC_{Re}$ region (C-terminal domain); and red, cross-domain (CD) region (N-terminal domain). Overall structure of $PhaC1_{Ps}$ (B). Cyan, N-terminal domain; orange, C-terminal domain; and red, CD region. (Left) Magnified images of catalytic residues (Cys315, Asp476, and His504) and beneficial site (Phe314) in $PhaC_{AR}$ and catalytic residues (Cys296, Asp451, and His 479) in

PhaC1$_{Ps}$. (Right) Magnified images of CD regions and Asn149 of PhaC$_{AR}$ and Glu130 of PhaC1$_{Ps}$. N396 and N372, which presumably interact with the beneficial positions 149 and 130, respectively, are highlighted.

Conclusions

Directed evolution of the sequence-regulating PHA synthase PhaC$_{AR}$ successfully increased activity toward the MCL substrate 3HHx-CoA. The F314H mutant is particularly useful because of high 3HHx incorporation and its capability to synthesize P(3HHx) homopolymer. The MCL PHA synthesized using class I PHA synthase had an advantage over that of class II enzymes in the polymer molecular weight, which was one order of magnitude higher (M_w ~10^6) than that obtained using a class II enzyme. In addition, these findings enabled us to synthesize a novel MCL-SCL PHA block copolymer P(3HHx)-*b*-P(2HB). The covalent linkage between the P(3HHx) and P(2HB) segments was verified by solvent fractionation. The predicted structure of PhaC$_{AR}$ by Alphafold2 suggests that there is a common mechanism among beneficial mutations in class I and II enzymes.

AUTHOR INFORMATION

Corresponding Author

* Ken'ichiro Matsumoto - Division of Applied Chemistry, Faculty of Engineering, Hokkaido University, Sapporo, Japan; https://orcid.org/0000-0002-5361-8352); Email: mken@eng.hokudai.ac.jp

Author Contributions

The manuscript was written through contributions of all authors. T.H.P. wrote the original draft and performed experiments. Y.H., M.G. and M.Y performed experiments. H.T. performed analysis and wrote paper. M.Z. partly supervise the project and wrote paper. K.M. designed experiments, supervise the project and wrote paper. All authors have given approval to the final version of the manuscript. ‡These authors contributed equally.

Notes

The authors declare no competing financial interest.

ACKNOWLEDGMENT

This work was supported by the JST-Mirai Program (No. JPMJMI19EB to K.M.), JSPS Kakenhi (20H04368 to K.M.), Grant for Basic Science Research Project from The Sumitomo Foundation (to H.T.), and the MOVE program at HES-SO Valais (to M.G. and M.Z.).

ABBREVIATIONS

AlkK, MCL 3-hydroxyalkanoic acid CoA ligase; CoA, coenzyme A ; ESI-MS, electrospray ionization-mass spectroscopy; GC, gas chromatography; HPLC, high-performance liquid chromatography; MCL, medium-chain-length; NMR, nuclear magnetic resonance; PCT, propionyl-CoA transferase; PHA, polyhydroxyalkanoate; PhaC, PHA synthase; SCL, short-chain-length; THF, tetrahydrofuran; 2HB, 2-hydroxybutyrate; 3HB, 3-hydroxybutyrate; 3HHx; 3-hydroxyhexanoate; P(2HB); poly(2-hydroxybutyrate); P(3HB), poly(3-hydroxybutyrate); P(3HHx), poly(3-hyrdroxyhexanoate)

REFERENCES

(1) Zinn, M.; Witholt, B.; Egli, T. Occurrence, synthesis and medical application of bacterial polyhydroxyalkanoate. *Adv. Drug Delivery. Rev.* **2001**, *53* (1), 5–21.

(2) Janes, B.; Hollar, J.; Dennis, D. Molecular characterization of the poly-ß-hydroxybutyrate biosynthetic pathway of *Alcaligenes eutrophus* H16. In *Novel Biodegradable Microbial Polymers*; Springer Netherlands, 1990; pp 175–190.

(3) El-malek, F. A.; Khairy, H.; Farag, A.; Omar, S. The sustainability of microbial bioplastics, production and applications. *Int. J. Biol. Macromol.* **2020**, *157*, 319–328.

(4) RameshKumar, S.; Shaiju, P.; O'Connor, K. E.; P, R. B. Bio-based and biodegradable polymers-state-of-the-art, challenges and emerging trends. *Green Sustainable. Chem.* **2020**, *21*, 75–81.

(5) Morohoshi, T.; Ogata, K.; Okura, T.; Sato, S. Molecular characterization of the bacterial community in biofilms for degradation of poly(3-hydroxybutyrate-*co*-3-hydroxyhexanoate) films in seawater. *Microbes Environ.* **2018**, *33* (1), 19–25.

(6) Sharma, P. K.; Munir, R. I.; Blunt, W.; Dartiailh, C.; Cheng, J.; Charles, T. C.; Levin, D. B. Synthesis and physical properties of polyhydroxyalkanoate polymers with different monomer compositions by recombinant *Pseudomonas putida* LS46 expressing a novel PHA synthase (PhaC116) enzyme. *Appl. Sci.* **2017**, *7* (3), 242.

(7) Tappel, R. C.; Wang, Q.; Nomura, C. T. Precise control of repeating unit composition in biodegradable poly(3-hydroxyalkanoate) polymers synthesized by *Escherichia coli*. *J. Biosci. Bioeng.* **2012**, *113* (4), 480–486.

(8) Hiroe, A.; Ishii, N.; Ishii, D.; Kabe, T.; Abe, H.; Iwata, T.; Tsuge, T. Uniformity of monomer composition and material properties of medium-chain-length polyhydroxyalkanoates biosynthesized from pure and crude fatty acids. *ACS Sustainable. Chem. Eng.* **2016**, *4* (12), 6905–6911.

(9) Chek, M. F.; Hiroe, A.; Hakoshima, T.; Sudesh, K.; Taguchi, S. PHA synthase (PhaC): interpreting the functions of bioplastic-producing enzyme from a structural perspective. *Appl. Microbiol. Biotechnol.* **2019**, *103* (3), 1131–1141.

(10) Kobayashi, G.; Shiotani, T.; Shima, Y.; Doi, Y. Biosynthesis and characterization of poly(3-hydroxybutyrate-*co*-3-hydroxyhexanoate) from oils and fats by *Aeromonas* sp. OL-338 and *Aeromonas* sp. FA-440. In *Biodegradable Plastics and Polymers*; Elsevier, 1994; Vol. 12, pp 410–416.

(11) Matsusaki, H.; Manji, S.; Taguchi, K.; Kato, M.; Fukui, T.; Doi, Y. Cloning and molecular analysis of the poly(3-hydroxybutyrate) and poly(3-hydroxybutyrate-*co*-3-hydroxyalkanoate) biosynthesis genes in *Pseudomonas* sp. strain 61-3. *J. Bacteriol.* **1998**, *180* (24), 6459–6467.

(12) Tripathi, L.; Wu, L. P.; Chen, J.; Chen, G. Q. Synthesis of diblock copolymer poly-3-hydroxybutyrate-*block*-poly-3-hydroxyhexanoate [PHB-*b*-PHHx] by a β-oxidation weakened *Pseudomonas putida* KT2442. *Microb. Cell Fact.* **2012**, *11* (1), 44.

(13) Pederson, E. N.; McChalicher, C. W. J.; Srienc, F. Bacterial synthesis of PHA block copolymers. *Biomacromolecules* **2006**, *7* (6), 1904–1911.

(14) Buckley, R. M.; Stubbe, J. Chemistry with an artificial primer of polyhydroxybutyrate synthase suggests a mechanism for chain termination. *Biochemistry* **2015**, *54* (12), 2117–2125.

(15) Matsumoto, K. K.; Hori, C.; Fujii, R.; Takaya, M.; Ooba, T.; Ooi, T.; Isono, T.; Satoh, T.; Taguchi, S. Dynamic changes of intracellular monomer levels regulate block sequence of polyhydroxyalkanoates in engineered *Escherichia coli*. *Biomacromolecules* **2018**, *19* (2), 662–671.

(16) Matsumoto, K.; Takase, K.; Yamamoto, Y.; Doi, Y.; Taguchi, S. Chimeric enzyme composed of polyhydroxyalkanoate (PHA) synthases from *Ralstonia eutropha* and *Aeromonas caviae* enhances production of phas in recombinant *Escherichia coli*. *Biomacromolecules* **2009**, *10* (4), 682–685.

(17) Matsumoto, K.; Terai, S.; Ishiyama, A.; Sun, J.; Kabe, T.; Song, Y.; Nduko, J. M.; Iwata, T.; Taguchi, S. One-pot microbial production, mechanical properties, and enzymatic degradation of isotactic P[(*R*)-2-hydroxybutyrate] and its copolymer with (*R*)-lactate. *Biomacromolecules* **2013**, *14* (6), 1913–1918.

(18) Kageyama, Y.; Tomita, H.; Isono, T.; Satoh, T.; Matsumoto, K. Artificial polyhydroxyalkanoate poly(2-hydroxybutyrate-*block*-3-hydroxybutyrate) elastomer-like material. *Sci. Rep.* **2021**, *11* (1), 22446.

(19) Feng, H.; Lu, X.; Wang, W.; Kang, N. G.; Mays, J. W. Block copolymers: synthesis, self-assembly, and applications. *Polym. (Basel, Switz.)* **2017**, *9* (10), 494.

(20) Taguchi, S.; Maehara, A.; Takase, K.; Nakahara, M.; Nakamura, H.; Doi, Y. Analysis of mutational effects of a polyhydroxybutyrate (PHB) polymerase on bacterial PHB accumulation using an *in vivo* assay system. *FEMS Microbiol. Lett.* **2001**, *198* (1), 65–71.

(21) Nomura, C. T.; Taguchi, S. PHA synthase engineering toward superbiocatalysts for custom-made biopolymers. *Appl. Microbiol. Biotechnol.* **2007**, *73* (5), 969–979.

(22) Wang, Q.; Tappel, R. C.; Zhu, C.; Nomura, C. T. Development of a new strategy for production of medium-chain-length polyhydroxyalkanoates by recombinant *Escherichia coli* via inexpensive non-fatty acid feedstocks. *Appl. Environ. Microbiol.* **2012**, *78* (2), 519–527.

(23) Spiekermann, P.; Rehm, B. H. A.; Kalscheuer, R.; Baumeister, D.; Steinbüchel, A. A sensitive, viable-colony staining method using Nile red for direct screening of bacteria that accumulate polyhydroxyalkanoic acids and other lipid storage compounds. *Arch. Microbiol.* **1999**, *171* (2), 73–80.

(24) Tomita, H.; Satoh, K.; Nomura, C. T.; Matsumoto, K. Biosynthesis of poly(glycolate-*co*-3-hydroxybutyrate-*co*-3-hydroxyhexanoate) in *Escherichia coli* expressing sequence-regulating polyhydroxyalkanoate synthase and medium-chain-length 3-hydroxyalkanoic acid coenzyme a ligase. *Biosci. Biotechnol. Biochem.* **2021**. *In Press*. DOI: 10.1093/bbb/zbab198.

(25) Minamoto, T.; Wada, E.; Shimizu, I. A new method for random mutagenesis by error-prone polymerase chain reaction using heavy water. *J. Biotechnol.* **2012**, *157* (1), 71–74.

(26) Hori, C.; Oishi, K.; Matsumoto, K.; Taguchi, S.; Ooi, T. Site-directed saturation mutagenesis of polyhydroxylalkanoate synthase for efficient microbial production of poly[(*R*)-2-hydroxybutyrate]. *J. Biosci. Bioeng.* **2018**, *125* (6), 632–636.

(27) Matsumoto, K.; Takase, K.; Aoki, E.; Doi, Y.; Taguchi, S. Synergistic effects of Glu130Asp substitution in the type II polyhydroxyalkanoate (PHA) synthase: enhancement of PHA production and alteration of polymer molecular weight. *Biomacromolecules* **2005**, *6* (1), 99–104.

(28) Kato, M.; Bao, H. J.; Kang, C. K. K.; Fukui, T.; Doi, Y. Production of a novel copolyester of 3-hydroxybutyric acid and medium-chain-length 3-hydroxyalkanoic acids by *Pseudomonas* sp. 61-3 from sugars. *Appl. Microbiol. Biotechnol.* **1996**, *45* (3), 363–370.

(29) Yamada, M.; Matsumoto, K.; Nakai, T.; Taguchi, S. Microbial production of lactate-enriched poly[(*R*)-lactate-*co*-(*R*)-3-hydroxybutyrate] with novel thermal properties. *Biomacromolecules* **2009**, *10* (4), 677–681.

(30) Matsumoto, K.; Shozui, F.; Satoh, Y.; Tajima, K.; Munekata, M.; Taguchi, S. Kinetic analysis of engineered polyhydroxyalkanoate synthases with broad substrate specificity. *Polym. J* **2009**, *41* (3), 237–240.

(31) Bradford, M. M. A rapid and sensitive method for the quantitation of microgram quantities of protein utilizing the principle of protein-dye binding. *Anal. Biochem.* **1976**, *72* (1), 248–254.

(32) Taguchi, S.; Nakamura, H.; Hiraishi, T.; Yamato, I.; Doi, Y. *In vitro* evolution of a polyhydroxybutyrate synthase by intragenic suppression-type mutagenesis. *J. Biochem.* **2002**, *131* (6), 801–806.

(33) Peter, D. M.; Vögeli, B.; Cortina, N. S.; Erb, T. J. A chemo-enzymatic road map to the synthesis of CoA esters. *Molecules* **2016**, *21* (4), 801–806.

(34) Takase, K.; Matsumoto, K.; Taguchi, S.; Doi, Y. Alteration of substrate chain-length specificity of type II synthase for polyhydroxyalkanoate biosynthesis by *in vitro* evolution: *in vivo* and *in vitro* enzyme assays. *Biomacromolecules* **2004**, *5* (2), 480–485.

(35) Curley, J. M.; and Baki Hazer; Lenz, R. W.; Fuller, R. C. Production of poly(3-hydroxyalkanoates) containing aromatic substituents by *Pseudomonas oleovorans*. *Macromolecules* **1996**, *29*, 1762–1766.

(36) Wu, B.; Lenz, R.; Hazer, B. Polymerization of methyl methacrylate and its copolymerization with ε-caprolactone catalyzed by isobutylalumoxane catalyst. *Macromolecules* **1999**, *32*, 6856–6859.

(37) Eisenberg, D.; Schwarz, E.; Komaromy, M.; Wall, R. Analysis of membrane and surface protein sequences with the hydrophobic moment plot. *J. Mol. Biol.* **1984**, *179* (1), 125–142.

(38) Wong, Y.-M.; Brigham, C. J.; Rha, C.; Sinskey, A. J.; Sudesh, K. Biosynthesis and characterization of polyhydroxyalkanoate containing high 3-hydroxyhexanoate monomer fraction from crude palm kernel oil by recombinant *Cupriavidus necator*. *Bioresour. Technol.* **2012**, *121*, 320–327.

(39) Kamiya, N.; Yamamoto, Y.; Inoue, Y.; Chujo, R.; Doi, Y. Microstructure of bacterially synthesized poly(3-hydroxybutyrate-*co*-3-hydroxyvalerate). *Macromolecules* **1989**, *22* (4), 1676–1682.

(40) Wang, H.; Zhou, X.; Liu, Q.; Chen, G. Biosynthesis of polyhydroxyalkanoate homopolymers by *Pseudomonas putida*. *Appl. Microbiol. Biotechnol.* **2011**, *89* (5), 1497–1507.

(41) Kichise, T.; Taguchi, S.; Doi, Y. Enhanced accumulation and changed monomer composition in polyhydroxyalkanoate (PHA) copolyester by *in vitro* evolution of *Aeromonas caviae* PHA synthase. *Appl. Environ. Microbiol.* **2002**, *68* (5), 2411–2419.

(42) Matsusaki, H.; Abe, H.; Doi, Y. Biosynthesis and properties of poly(3-hydroxybutyrate-*co*-3-hydroxyalkanoates) by recombinant strains of *Pseudomonas* sp. 61-3. *Biomacromolecules* **2000**, *1* (1), 17–22.

(43) Harada, K.; Kobayashi, S.; Oshima, K.; Yoshida, S.; Tsuge, T.; Sato, S. Engineering of *Aeromonas caviae* polyhydroxyalkanoate synthase through site-directed mutagenesis for enhanced polymerization of the 3-hydroxyhexanoate unit. *Front. Bioeng. Biotechnol.* **2021**, *9* (March), 627082.

(44) Yuan, W.; Jia, Y.; Tian, J.; Snell, K. D.; Müh, U.; Sinskey, A. J.; Lambalot, R. H.; Walsh, C. T.; Stubbe, J. Class I and III polyhydroxyalkanoate synthases from *Ralstonia eutropha* and *Allochromatium vinosum*: characterization and substrate specificity studies. *Arch. Biochem. Biophys.* **2001**, *394* (1), 87–98.

(45) Cramer, P. AlphaFold2 and the future of structural biology. *Nat. Struct. Mol. Biol.* **2021**, *28* (9), 704–705.

(46) Wittenborn, E. C.; Jost, M.; Wei, Y.; Stubbe, J. A.; Drennan, C. L. Structure of the catalytic domain of the class I polyhydroxybutyrate synthase from *Cupriavidus necator*. *J. Biol. Chem.* **2016**, *291* (48), 25264–25277.

(47) Chek, M. F.; Kim, S. Y.; Mori, T.; Arsad, H.; Samian, M. R.; Sudesh, K.; Hakoshima, T. Structure of polyhydroxyalkanoate (PHA) synthase PhaC from *Chromobacterium* sp. USM2, producing biodegradable plastics. *Sci. Rep.* **2017**, *7* (1), 5312.

(48) Chek, M. F.; Kim, S. Y.; Mori, T.; Tan, H. T.; Sudesh, K.; Hakoshima, T. Asymmetric open-closed dimer mechanism of polyhydroxyalkanoate synthase PhaC. *iScience* **2020**, *23* (5), 101084.

(49) Lim, H.; Chuah, J.-A.; Chek, M. F.; Tan, H. T.; Hakoshima, T.; Sudesh, K. Identification of regions affecting enzyme activity, substrate binding, dimer stabilization and polyhydroxyalkanoate (PHA) granule morphology in the PHA synthase of *Aquitalea* sp. USM4. *Int. J. Biol. Macromol.* **2021**, *186*, 414–423.

(50) Kim, Y.-J.; Choi, S. Y.; Kim, J.; Jin, K. S.; Lee, S. Y.; Kim, K.-J. Structure and function of the N-terminal domain of *Ralstonia eutropha* polyhydroxyalkanoate synthase, and the proposed structure and mechanisms of the whole enzyme. *Biotechnol. J.* **2017**, *12* (1), 1600649.

Table of Contents graphics